

Reaction mechanisms of the thermal conversion of Pu(IV) oxalate into plutonium oxide

N. Vigier^a, S. Grandjean^{a,*}, B. Arab-Chapelet^a, F. Abraham^b

^a CEA Valrhô Marcoule, DRCP/SCPS/LCA, Bât 399, BP 17171, 30207 Bagnols-sur-Cèze, France

^b UCCS – Équipe Chimie du Solide, UMR CNRS 8181, ENSCL-USTL, BP 108, 59652 Villeneuve-d'Ascq Cedex, France

Received 28 June 2006; received in revised form 8 January 2007; accepted 12 January 2007

Available online 18 January 2007

Abstract

During the oxalic conversion of plutonium into oxide at the end of the PUREX process, the thermal transition of Pu(IV) oxalate into oxide plays a significant role leading to the main properties of the oxide. The structure of the solid intermediates is often speculative and the reaction mechanisms are quite misunderstood and divergent from one study to another. This work deals with a detailed structural investigation on the main solid intermediates encountered when calcining Pu(IV) oxalate into oxide under air or argon.

© 2007 Elsevier B.V. All rights reserved.

Keywords: Actinide alloys and compounds; Oxide materials; Solid state reactions; Phase transitions; Thermal analysis

1. Introduction

The conversion of actinide nitrates into actinide oxides for the treatment of solution containing actinides is the method of choice in the nuclear industry with the intent to immobilize them into a ceramic phase for long-term storage or prior to their recycling into a new fuel. Noticeably, dealing with the recycling of the valuable actinides contained in the used fuel, the oxalic conversion of plutonium into oxide at the end of the PUREX process is one of the most important steps. If the oxalic precipitating step is a key-operation leading to the first solid phase, the thermal transition of Pu(IV) oxalate into oxide plays a significant role leading to important properties of the oxide powder: open/closed porosities, specific area, residual carbon concentration. The overall control of these properties is relatively well achieved by choosing conveniently the maximal temperature during the heating. Specific area of plutonium oxide for example depends quite directly on the maximal temperature reached during the heating step of the conversion [1]. On the contrary, the first steps of the decomposition imposed by the thermal program are often neglected even if they can sig-

nificantly influence the total carbon departure from the solid phase, the creation of porosities, even the potential formation of fine solid fractions when the solid particles burst from thermal stress.

However, the structure of the intermediates during the oxalic conversion of Pu(IV) into oxide is often speculative and the reaction mechanisms are quite misunderstood and divergent from one study to another [2–8]. This work deals with a detailed structural investigation on the main solid intermediates formed when calcining Pu(IV) oxalate into oxide under air or argon.

2. Experimental methods

2.1. Preparation of the Pu(IV) oxalate

The Pu(IV) oxalate precipitate, $\text{Pu}^{\text{IV}}(\text{C}_2\text{O}_4)_2 \cdot 6\text{H}_2\text{O}$, was prepared extemporaneously by mixing an acid Pu(IV) nitrate solution and a concentrated $\text{H}_2\text{C}_2\text{O}_4$ solution in a vortex effect reactor with a slight excess of $\text{H}_2\text{C}_2\text{O}_4$. The resulting crystallized powder was filtered off, washed with a 90/10 ethanol/water solution and dried at room temperature.

2.2. Analytical methods

Thermogravimetric analyses (TG) were carried out with a NETZSCH STA 409C analyzer under argon flow or static air, at a constant rate of 2°C min^{-1} up to 700°C . Samples of oxalate weighing approximately 40 mg were placed in an 85 μL alumina crucible. A lid with a pinhole was fitted on the crucible for the

* Corresponding author. Tel.: +33 4 66 79 16 03; fax: +33 4 66 79 65 67.
E-mail address: stephane.grandjean@cea.fr (S. Grandjean).

analyses under Ar flow in order to avoid material loss (micrometric particles) when evacuating residual air from the furnace. Using the same procedure, solid intermediates were isolated at specific temperatures for immediate structural investigations.

X-ray powder diffraction (XRD) data were acquired with an INEL CPS 120 diffractometer (curved position sensitive detector) using Cu $K\alpha_1$ radiation isolated by a Ge monochromator. Si or Au was used as internal standards. Each solid sample was mixed into an epoxy resin in order to minimize contamination. UV–vis spectra of the solid intermediates and products were acquired between 400 and 800 nm with a HITACHI U-3000 analyzer equipped with an integration sphere. Infrared (IR) spectra of all samples were recorded with a NICOLET MAGNA IR 550 series II. A spectral range from 400 to 4000 cm^{-1} was typically investigated.

3. Results

A typical TG plot is shown in Fig. 1 (static air). Each intermediate was identified by extrapolating the molecular formula from the mass loss, and/or by structural analyses (XRD, UV–vis, IR) of the isolated solid after stopping the heating at the corresponding temperature (see Figs. 2 and 3).

XRD investigations confirm the identity of the crystallized intermediate compounds, that is, the hexa- and di-hydrated oxalate structures and the final oxide: each powder diffractogram conforms to the compiled JCPDS data. Attempts to isolate singly

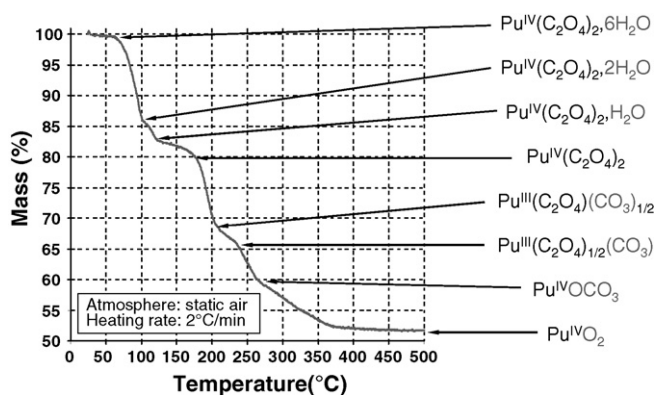


Fig. 1. TG plot starting from a $\text{Pu}^{\text{IV}}(\text{C}_2\text{O}_4)_2 \cdot 6\text{H}_2\text{O}$ sample under static air.

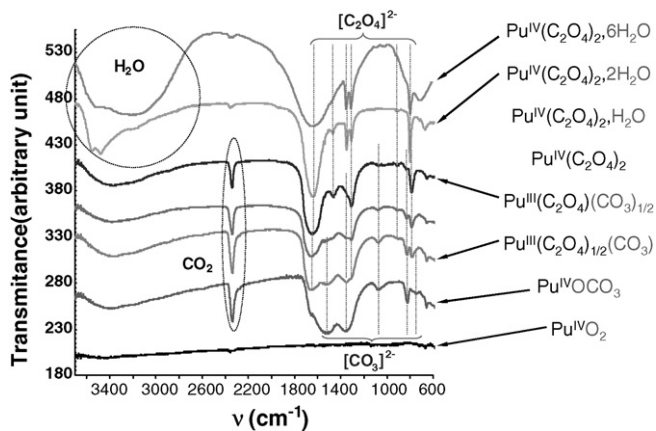


Fig. 2. Infrared spectra of the intermediate products of the $\text{Pu}^{\text{IV}}(\text{C}_2\text{O}_4)_2 \cdot 6\text{H}_2\text{O}$ decomposition under static air isolated at the intermediate stages specified in Fig. 1.

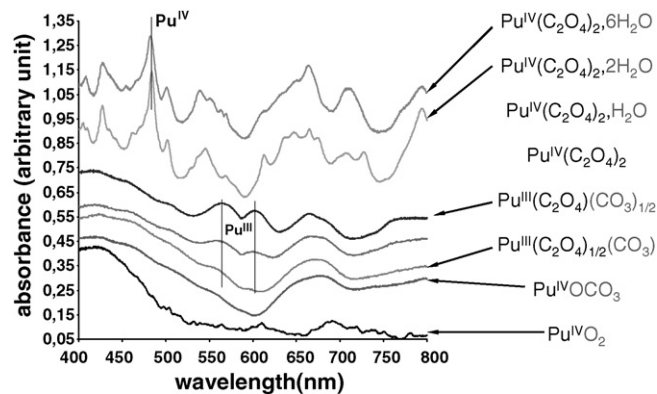


Fig. 3. UV–vis spectra of the intermediate products of the $\text{Pu}^{\text{IV}}(\text{C}_2\text{O}_4)_2 \cdot 6\text{H}_2\text{O}$ decomposition under static air isolated at the intermediate stages specified in Fig. 1.

hydrated Pu(IV) oxalate and the anhydrous Pu(IV) oxalate failed due to fast partial hydration of these compounds.

IR spectra (Fig. 2) permits the identification of the exact beginning of the decomposition of the oxalate entities and the successive replacement of oxalate anions by carbonate ones up to the build-up of Pu(IV) oxy-carbonate. Occlusion or sorption of CO_2 in the solid is certainly responsible for the band observed around 2350 cm^{-1} ($\nu_3\text{ CO}_2$ band). The observation of this band was often mentioned previously [6,7,9], but no explanation was given.

Direct UV–vis spectra of the solids shown on Fig. 3 highlight the total reduction of the Pu(IV) to Pu(III), even under air atmosphere, after the total dehydration of the oxalate and as soon as oxalate–carbonate structures begin to form. After total decomposition of the oxalate, Pu(III) is oxidized again to the fourth oxidation state, even if it cannot be ascertained strictly by UV–vis spectra.

The same investigations were conducted using Ar atmosphere instead of air. A typical TG plot as obtained utilizing an Ar atmosphere is shown on Fig. 4 and compared with that obtained under static air. If transitory plutonium reduction is observed using both atmospheres, then the nature of the corresponding Pu(III) solid intermediate(s) was found significantly different (Fig. 5). IR spectra of the intermediates obtained in inert atmosphere show only oxalate specific bands and mass loss, also the direct UV–vis spectrum (not repre-

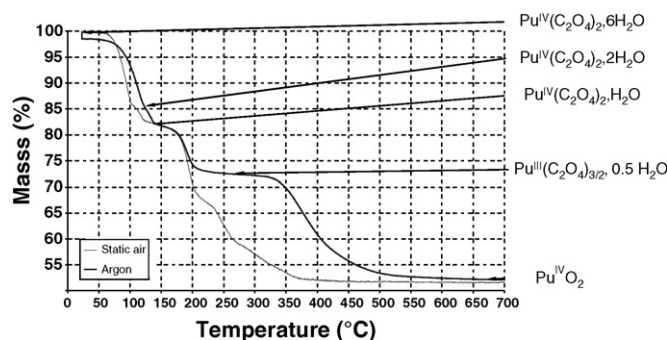


Fig. 4. TG plot starting from a $\text{Pu}^{\text{IV}}(\text{C}_2\text{O}_4)_2 \cdot 6\text{H}_2\text{O}$ sample under argon.

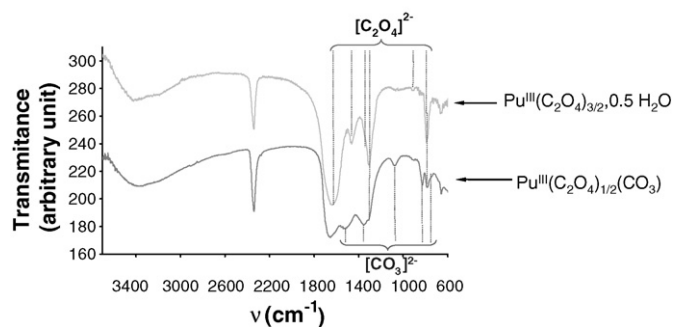


Fig. 5. Comparison of the infrared spectra of the Pu(III) intermediate products formed during $\text{Pu}^{\text{IV}}(\text{C}_2\text{O}_4)_2 \cdot 6\text{H}_2\text{O}$ decomposition under static air or under Ar.

sented), are consistent with the formula $\text{Pu}_2^{\text{III}}(\text{C}_2\text{O}_4)_3 \cdot \text{H}_2\text{O}$ for this compound. On the TG plot, the decomposition of this intermediate appears continuous up to the formation of the oxide (i.e. from 320 up to 600 °C), without stabilization of any precise intermediate.

4. Discussion

The proposed reaction mechanism leading to plutonium oxide under air is detailed in Fig. 6.

Under air, the transitory reduction of Pu(IV) into Pu(III) is for the first time established directly by structural analysis of the solid intermediates: the Pu(III) intermediates are mixed oxalate–carbonate structures, confirming previous hypotheses of Rao et al. [3], and not anhydrous Pu(III) oxalate as sometimes described [2,6–8]. The UV–vis spectra of the first solid intermediates after dehydration of the Pu(IV) oxalate highlight indeed a total and quite durable reduction of the Pu(IV) to Pu(III). This result excludes an artefact due to a lack of free access of oxygen in the solid as previously stated [5], particularly considering the slow heating rate (2 °C min⁻¹) used in the present study, but confirms the stabilization of real transient Pu(III) intermediates after reaction of the anhydrous Pu(IV) residue with in situ formed carbon monoxide. The progressive increase of the 830 cm⁻¹ carbonate $\pi(\text{CO}_3)$ band and the simultaneous decrease of the 800 cm⁻¹ oxalate $\delta(\text{OCO})$ one for example [10], demonstrate the progressive replacement of oxalate entities by carbonate ones in

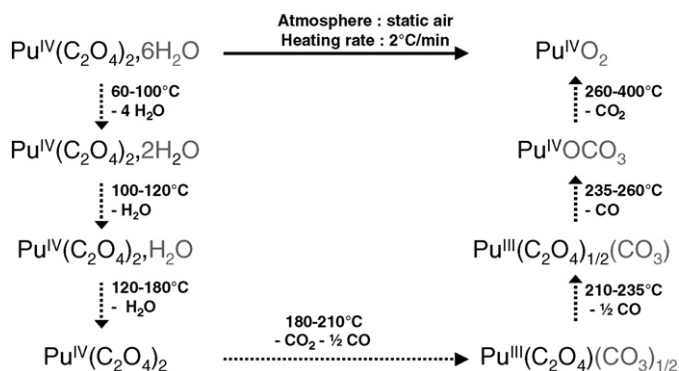


Fig. 6. Reaction path of the thermal conversion of $\text{Pu}^{\text{IV}}(\text{C}_2\text{O}_4)_2 \cdot 6\text{H}_2\text{O}$ into oxide under air.

the Pu(III) intermediates $\text{Pu}_2^{\text{III}}(\text{C}_2\text{O}_4)_{3-x}(\text{CO}_3)_x$ ($x = 1-2$) when increasing temperature. Transitory formation of $\text{Pu}_2^{\text{III}}(\text{C}_2\text{O}_4)_3 \cdot 0-1 \text{H}_2\text{O}$ is not observed, and if it does form then it would be very transient.

The schematic path under argon differs mainly from that obtained under air by the formation of a distinct major Pu(III) intermediate, the Pu(III) oxalate $\text{Pu}_2^{\text{III}}(\text{C}_2\text{O}_4)_3 \cdot \text{H}_2\text{O}$ which is particularly stable in temperature from 220 up to 320 °C (in the conditions of the present study), as compared with the Pu(III) oxalate–carbonate intermediates $\text{Pu}_2^{\text{III}}(\text{C}_2\text{O}_4)_{3-x}(\text{CO}_3)_x$ ($x = 1-2$) formed under air.

These distinct reaction paths under air or argon are responsible for a significantly different specific surface area of the corresponding oxide powder obtained at 650 °C using the above described conditions: around 11 and 20 m²/g, respectively, from BET measurements. The main steps involving the decomposition of the oxalate groups after dehydration of the solids are accompanied by distinct sequencing release of CO or CO₂. Noticeably the formation of the oxide is complete at around 400 °C under air and at around 600 °C under Ar.

It should be noted that the powder obtained at 650 °C under Ar contains up to 1% weight elemental carbon (evaluated by TG analysis, after heating the powder under air up to 1000 °C), whose formation originates from the complex redox behaviour of CO under an inert atmosphere.

Two intermediates, $\text{Pu}^{\text{IV}}(\text{C}_2\text{O}_4)_2 \cdot \text{H}_2\text{O}$ and $\text{Pu}^{\text{IV}}(\text{C}_2\text{O}_4)_2$, were not strictly identified due to their particular instability in ambient conditions: the first one reacts with trace amounts of water to form again $\text{Pu}^{\text{IV}}(\text{C}_2\text{O}_4)_2 \cdot 2\text{H}_2\text{O}$. The crystal structure of the last cited compound and the high temperature XRD with other in situ investigations of the mono-hydrated and anhydrous oxalates are planned.

5. Conclusion

The reaction mechanism of the thermal treatment of $\text{Pu}^{\text{IV}}(\text{C}_2\text{O}_4)_2 \cdot 6\text{H}_2\text{O}$ into oxide under air or argon was thoroughly investigated using TG analysis and structural analysis of the solid intermediates. Distinct reaction paths were established depending on the atmosphere used. The identity of some intermediates was assessed comparatively to previous studies and uncertainties about the Pu(III) intermediates formed, either under air or argon, were clarified.

Acknowledgements

This research was financially supported by AREVA NC, France. We thank J.-L. Emin, AREVA NC, France, for encouraging this work and for fruitful discussions.

References

- [1] X. Machuron-Mandard, C. Madic, J. Alloys Compd. 235 (1996) 216–224.
- [2] M.N. Myers, U.S.A.E.C. document HW 45128, 1956.
- [3] G.S. Rao, M.S. Subramanian, G.A. Welch, J. Inorg. Nucl. Chem. 25 (1963) 1293–1295.

- [4] I.L. Jenkins, M.J. Waterman, J. Inorg. Nucl. Chem. 26 (1964) 131–137.
- [5] A. Glasner, J. Inorg. Nucl. Chem. 26 (1964) 1475–1476.
- [6] D.A. Nissen, J. Therm. Anal. 18 (1980) 99–109.
- [7] R.D. Kozlova, A.I. Karelin, O.P. Lobas, V.A. Matyukha, Radiokhimiya 26 (3) (1984) 311–316.
- [8] A.I. Karelin, N.N. Krot, R.D. Kozlova, O.P. Lobas, V.A. Matyukha, J. Radioanal. Nucl. Chem. 143 (1) (1990) 241–252.
- [9] B.A.A. Balboul, A.M. El-Roudi, E. Samir, A.G. Othman, Thermochim. Acta 387 (2002) 109–114.
- [10] K. Nakamoto, Infrared and Raman Spectra of Inorganic and Coordination Compounds, 3rd ed., 1978.